



Petrographic and geochemical analyses of Late Bronze and Iron Age pottery from Arslantepe (Malatya, Turkey): insights into the local organization of the production and extra-regional networks of exchange

Pamela Fragnoli¹ · Federico Manuelli^{2,3}

Received: 31 March 2023 / Accepted: 1 June 2023 / Published online: 11 July 2023
© The Author(s) 2023

Abstract

In this paper, we analyzed Late Bronze and Iron Age pottery assemblages from the site of Arslantepe (Malatya, eastern Turkey) by utilizing a combination of thin-section petrography and X-ray wavelength dispersive fluorescence techniques. Following an introduction to the site and an overview of the archeological and historical evidence, the analysis is presented, and the outcomes discussed in the wider framework of the Syro-Anatolian and eastern Mediterranean regions. The results show elements of both continuity and change over the second millennium and until the beginning of the first millennium BC. On a local level, the use of volcanic-based recipes for the production of painted vessels represents the most striking element of continuity. In contrast, noteworthy elements of changes relate to an increased exploitation of geological deposits south of Arslantepe and the standardization of paste recipes for cooking pots. Remarkable results also pertain to extra-regional exchanges: The Late Bronze Age Red Lustrous Wheel-made Ware found at the site is imported from Cilicia, while the wares of foreign tradition from the Middle Iron Age levels are mostly locally produced.

Keywords Late Bronze Age · Iron Age · Arslantepe · Pottery · Petrography · Geochemistry

Introduction

Arslantepe is a multi-stratified mound of approximately 4.5 ha located in south-eastern Anatolia a few kilometers west of the Euphrates river (Malatya, Turkey) (Fig. 1). The excavations conducted continuously since 1961 by the Italian Archeological Expedition in Eastern Anatolia from Sapienza University of Rome (MAIAO) allowed the discovery of a long and detailed sequence, mostly anchored to high precision 14C dating stretching from the end of the

fifth millennium BC to the Byzantine era (Frangipane 2019; Vignola et al. 2019; Manuelli et al. 2021).

Investigations into the Late Bronze and Iron Age levels have been conducted intermittently at the site. The first activities of the Italian expedition were carried out on the northern sector, in the area where a French team directed by Louis Delaporte had brought to light during the 1930s the remains of the famous “Lions Gate” (Delaporte 1940). Here, a sequence of monumental structures, which spans from the sixteenth to the tenth centuries BC, were investigated for over 10 years (Pecorella 1975; Palmieri 1973: 65–80; Palmieri 1978a; Manuelli 2013: 39–48). In 1971, the beginning of the activities on the southern sector marked the interruption of the large-scale investigations of the historical levels; nonetheless, a significant series of Late Bronze Age 1 domestic structures, dated to the seventeenth and sixteenth centuries BC, have been unearthed over the years (Palmieri 1973: 65–66; Frangipane and Palmieri 1983: 288–290; Manuelli 2013: 48–71). After more than 40 years of inactivity, a new round of investigations of the northern sector started in 2008 with the aim of finally providing answers about the development

✉ Pamela Fragnoli
pamela.fragnoli@oeaw.ac.at

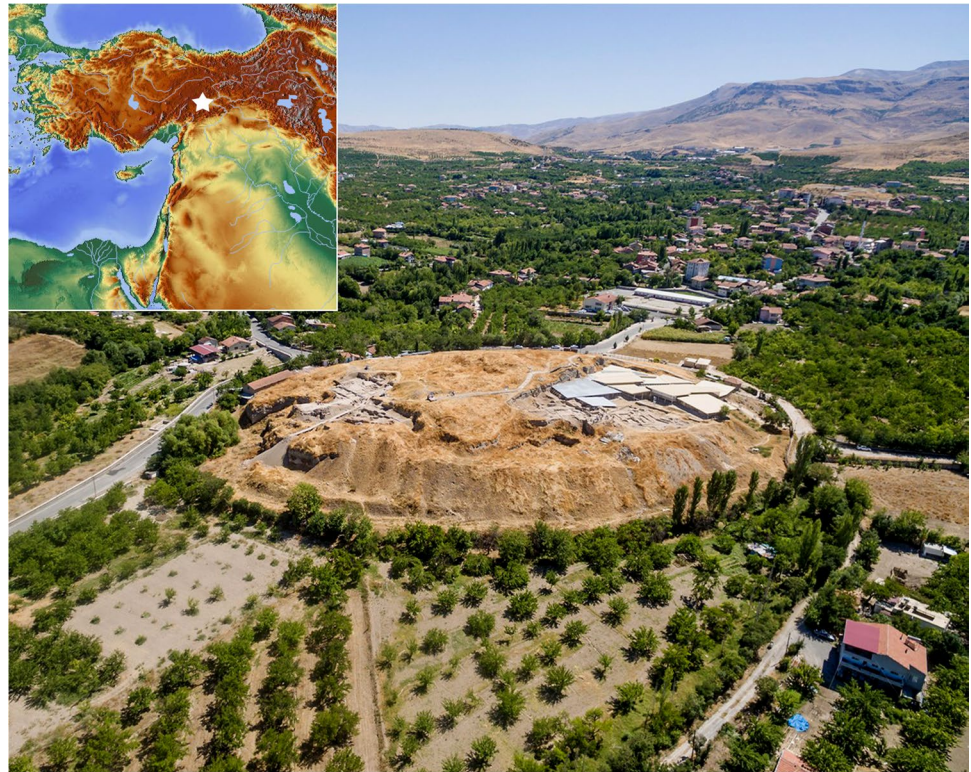
Federico Manuelli
federico.manuelli@cnr.it; federico.manuelli@fu-berlin.de

¹ Austrian Archaeological Institute, Austrian Academy of Sciences, Vienna, Austria

² Institute of Heritage Science (ISPC), Italian National Research Council (CNR), Rome, Italy

³ Institut für Altorientalistik, Freie Universität Berlin, Berlin, Germany

Fig. 1 The site of Arslantepe and the Malatya plain from north-west. The Late Bronze and Iron Age sectors are visible on the left (photo ©MAIAO). In the upper box, the geographical position of the site is highlighted (map courtesy of Maps for Free, elaborated by the authors)



of the site during the second and first millennium BC (Liverani 2012). Excavations carried out until 2010 and later in 2015 and 2016 have been conducted over a large area, leading to the discovery of an uninterrupted sequence from the mid-thirteenth to the seventh century BC (Manuelli et al. 2021). In 2016, a new area was opened with the aim of connecting the northern sector with the inner part of the settlement. Ongoing excavations have brought to light monumental remains that can be dated between the tenth and the seventh century BC (Frangipane et al. 2020).

The pottery repertoire from Arslantepe has been for decades an object of archaeometric analysis, mainly consisting in thin-section petrography and wavelength dispersive X-ray fluorescence. The ceramic samples analyzed so far cover a chronological span of almost 4 millennia from the Late Chalcolithic to the Middle Iron Age. Coupled with raw material surveys and technological observations, these analyses evidenced diachronic variations in the organization of production in relation to different levels of socio-economic complexity (Fragoli and Palmieri 2017; Fragoli 2018; Fragoli and Frangipane 2022).

In this paper, we present the results of petrographic and geochemical analyses recently carried out on 99 samples (Table 1) from well-contextualized Late Bronze and Iron Age pottery assemblages from the site. Considering the wide time-frame covered by this research as well as the manifold historical implications related to the

abovementioned periods, this analysis is not meant to deal comprehensively with all the questions that might be raised by the study of each ware class involved. Rather, it intends to provide an overview of the results obtained so far and new food for thought for future discussions. Physical and chemical analyses have been widely carried out on pottery assemblages at many Late Bronze and Iron Age key-sites of the eastern Mediterranean world. However, the specific situation of the Upper Euphrates is instead very fragmented, and comparisons need to be found in the wider framework of the Syro-Anatolian region.

With this in mind, the main aim of this study is to highlight elements of continuity and discontinuity in both paste recipes and material supply as well as potential diachronic changes in manufacturing techniques and the organization of the production at the Late Bronze-Iron Age transition. We also seek to better comprehend the impact that certain exogenous ware classes have had on the local production over the centuries, with a specific focus on the Middle Iron Age.

Archeological and historical overview

During the Late Bronze Age Arslantepe was affected by the Hittite imperial military expansion. The campaigns of the Hittite kings succeeded in subjugating the

Table 1 List of the ceramic samples analyzed in the paper with respective phases, wares, descriptions, contexts and petrographic groups

Sample	Phase	Ware classes	Description of the forms	Context	Petro group	XRFWDS
326/2015	VB1	B1	Necked medium-sized jar (#521)	D9(12)(16) A1200 X7	CEa	
329/2015	VB1	E1	Necked pithos with drip marks (#718)	D10(1–4) A1200 X6	VCEm-a	✓
328/2017	VB1	E1	Necked pithos with drip marks (#718)	D10(1–4) A1200 X6	VCEm-a	
333/2015	VB1	D1	Shallow hemispherical bowl (#531)	D9(12)(16) A1200 1a	CIb	
335/2015	VB1	A2	Short-necked medium-sized cooking pot (#68)	D9(11)(15) A237 X7	NC	
336/2015	VB1	D1	High-necked large-sized bottle (#149)	D9(13) A140 X1	CEa-m + Ib	✓
337/2015	VB1	B1	High-necked large-sized jar (#69)	D9(11–15) A250 X1	VCEa	
342/2015	VB1	E2	Neckless pithos (#695)	D9(14–15) A257 X16	NC	✓
343/2015	VB1	C1	Necked mug (#519)	D9(12)(16) A1200 X8	CIb	
346/2017	VB1	C1	Jar with painted bands pattern	D10(1–4) A1200 2a*	CEm-a	✓
328/2015	VB2	C3	Ring base (#52)	D9(13)(14) A141 2a	Mgne + serp + metag + sc	
330/2015	VB2	D2	High-necked large-sized bottle (#118)	D9(13) A140 1a	CEb-m	
331/2015	VB2	A1	Short-necked medium-sized cooking pot (#194)	D9(16) A1200 X3	NC	✓
332/2015	VB2	A1	Neckless small-sized cooking pot (#404)	C3(F2) Vd	Ia + Ib	
338/2015	VB2	E1	Necked pithos (#715)	C3(P1) Vd	VCEm-a	✓
346/2015	VB2	C2	Necked small-sized jar (#83)	D9(9–10) K73 1c	CEa	
340/2017	VB2	C2	Jar with painted cross-hatching pattern (#778)	C3(F1) Va	CEm-a	
341/2017	VB2	D2	High-necked large-sized jar with painted bands pattern (#769)	C3(F1) Vb	CEb-m	
347/2017	VB2	D2	Bowl with decorative slip	D9(13–14) A141 2a	CEb-m	
340/2015	VB-IV	F1	Arm-shaped vessel (#848)	D9(14) 1d	Q	
329/2017	VB-IV	F1	Arm-shaped vessel (#848)	D9(14) 1d	VCEm-a	✓
327/2015	IV	A2	Neckless medium-sized cooking pot (#409)	C3(F3) Va*	Mgne + serp + metag + sc	✓
334/2015	IV	F1	Pedestal base (#57)	C3(F1) Va	Q	
332/2017	IV	F1	Pedestal base (#57)	C3(F1) Va	/	✓
339/2015	IV	E2	Necked pithos with drip marks (#717)	C3(D) IVc	VCEm-a	✓
337/2017	IV	E2	Necked pithos with drip marks (#717)	C3(D) IVc	VCEm-a	
341/2015	IV	F1	High-necked small-sized bottle	C3(F3) IVb	Q	
336/2017	IV	F1	High-necked small-sized bottle	C3(F3) IVb	/	✓
344/2015	IV	D2	Flat bowl (#324)	C3(F1) Va	CEb-m	✓
345/2015	IV	C3	Flat bowl (#319)	C3(F3) Va	VCEa-m + Ib	
347/2015	IV	C2	Flat bowl (#279)	C3(F4) Iva	NC	
348/2015	IV	C1	Flat bowl (#271)	C3(F3) Va*	Mgne + serp + metag + sc	
344/2017	IV	D2	Necked small-sized jar with painted cross pattern (#782)	C3(F1) IVc*	CEb-m	
345/2017	IV	D2	Jar with painted triangles pattern (#777)	C3(F2) IV	CEb-m	
348/2017	IV	D2	Jar with painted angled pattern (#781)	C3(F4) IVb	CEb-m	✓
349/2017	IV	C2	Bowl with decorative slip	C3(F1) IVb	CEm-a	
305/2015	IIIA	K1	Neckless large-sized cooking pot (#45)	C3(A) IIIc	Ia + Ib	
306/2015	IIIA	K1	Bottle (#266)	G3(11) A1279 1b	NC	
296/2017	IIIA	K1	Neckless large-sized cooking pot (#34)	C3(F3) III e*	CEa-m + Ib	
307/2015	IIIA	K1	Neckless large-sized cooking pot (#34)	C3(F3) IIIe*	VCMgne + metag + Ib	
308/2015	IIIA	K2	Neckless small-sized cooking pot (#319)	G3(11) A1278 rP1	VCMgne + metag + Ib	
309/2015	IIIA	P1	Neckless pithos (#72)	C3(F3) IIIId	VCEa-m + Ib	✓
310/2015	IIIA	P1	Necked pithos (#279)	G3(11) A1279 1a	VCMgne + metag + Ib	✓
311/2015	IIIA	P1	Bottle (#94)	C3(F1) IIIb	VCMgne + metag + Ib	
312/2015	IIIA	K1	Neckless small-sized cooking pot (#283)	G3(11) A1279 1a	VCMgne + metag + Ib	
307/2017	IIIA	K1	Neckless small-sized cooking pot (#283)	G3(11) A1279 1a	CIa + Ib	

Table 1 (continued)

Sample	Phase	Ware classes	Description of the forms	Context	Petro group	XRFWDS
313/2015	IIIA	K2	Short-necked small-sized cooking pot (#298)	G3 (11) A1279 1c	VCMgne + metag + Ib	✓
314/2015	IIIA	P1	Krater (#238)	G3(11) A1279 1c	VCMgne + metag + Ib	
294/2017	IIIA	S2	Necked large-sized jar (#58)	C3(F2) III d*	CIa + Ib	
315/2015	IIIA	S2	Necked large-sized jar (#58)	C3(F2) III d*	VCIb	
317/2017	IIIA	S2	Flat bowl (#166)	G3(11) A1279 1c	CIa + Ib	
316/2015	IIIA	S2	Flat bowl (#166)	G3(11) A1279 1c	VCMgne + metag + Ib	
317/2015	IIIA	S2	Flat bowl (#182)	G3(11) A1279 2a	VCEa-m + Ib	
313/2017	IIIA	S2	Flask (#57)	G3(F2) III d*	VCMgne + metag + Ib	
318/2015	IIIA	S2	Flask (#57)	C3(F2) III d*	VCMgne + metag + Ib	
312/2017	IIIA	S3	Necked large-sized jar (#243)	G3(11) A1279 1a	CIb	
319/2015	IIIA	S3	Necked large-sized jar (#243)	G3(11) A1279 1a	VCMgne + metag + Ib	
320/2015	IIIA	S3	Jar (#74)	C3(F3) III f	VCEa-m + Ib	
295/2017	IIIA	S3	Bottle (#249)	G3(11) A1279 1b	CMgne + metag + metaub	
321/2015	IIIA	S3	Bottle (#249)	G3(11) A1279 1b	CMgne + metag + metaub	
299/2017	IIIA	S1	Flat bowl (#174)	G3(11) A1279 1b	VCIa	
322/2015	IIIA	S1	Flat bowl (#174)	G3(11) A1279 1b	VCIa	
298/2017	IIIA	S1	Flat bowl (#187)	G3(11) A1278 rP1	VCIa	
323/2015	IIIA	S1	Flat bowl (#187)	G3(11) A1278 rP1	VCIa	
324/2015	IIIA	P2	Neckless pithos (#277)	G3(11) A1278 rP1	VCMgne + metag + Ib	✓
325/2015	IIIA	P2	Necked pithos (#101)	C3(F2) III d*	NC	✓
297/2017	IIIA	S2	Flat bowl (#530)	G3(14) A1426 4a*	NC	
300/2017	IIIA	K2	Neckless small-sized cooking pot (#319)	G3(11) A1278 rP1	VCMgne + metag + Ib	
301/2017	IIIA	S1	Flat bowl (#1208)	G3(13) A1421 rP1	CEa-m + Ib	✓
302/2017	IIIA	K1	Neckless large-sized cooking pot (#45)	C3(A) III c	Ia + Ib	
303/2017	IIIA	P2	Krater (#1106)	G3(10–11) 9a	CMgne + metag + metaub	
304/2017	IIIA	S1	Flat bowl (#840)	G3(14) A1426 2a	VCIa	
305/2017	IIIA	S2	Flat bowl (#182)	G3(11) A1279 2a	CEa-m + Ib	✓
306/2017	IIIA	P1	Krater (#238)	G3(11) A1279 1c	VCMgne + metag + Ib	
308/2017	IIIA	S2	Short-necked large-sized cooking pot (#922)	G3(13) A1421 2a*	VCMgne + metag + Ib	
309/2017	IIIA	P1	Pithos (#867)	G3(14) A1423 X1	CIa + Ib	
310/2017	IIIA	F1	Flat bowl (#909)	G3(14) A1423 1a*	CIb	
311/2017	IIIA	S1	Flat bowl (#519)	G3(14) A1426 3a	VCIa	✓
314/2017	IIIA	S3	Necked large-sized jar (#950)	G3(13) A1421 1a*	CMgne + metag + metaub	
315/2017	IIIA	S1	Flat bowl (#545)	G3(10) A1436 2a	CIa + Ib	
316/2017	IIIA	K1	Neckless small-sized cooking pot (#556)	G3(10) A1436 2a	VCMgne + metag + Ib	
349/2015	IIA	IN	Jar (#409)	F3(16) A1168 1a	VCEa-m + Ib	✓
350/2015	IIA	GW	Carinated big bowl (#402)	G3(14) A1168 2a	NC	
351/2015	IIA	RB	Bowl	G4(2) A1168 1a	VCIb	
352/2015	IIA	RB	Big bowl (#408)	G4(2) A1168 1a	CIb	✓
353/2015	IIA	AL	Jar (#423)	F3(16)F4(4) A1168 2c	VCEa-m + Ib	✓
354/2015	IIA	AB	Necked jar (#424)	F3(15) rM169	CEb-m	✓
355/2015	IIA	AB	Jar	F3(14) A1139 rP2	NC	
356/2015	IIA	RS	Bowl	G3(14) A1168 2a*	CEa-m + Ib	✓
357/2015	IIA	CP	Jar (#429)	G4(2) A1168 1a	VCIb	
359/2015	IIA	CP	Jar	G3(14) A1168 2a	CIb	✓
318/2017	IIA	RS	Bowl	H4(15) A1435 rP2	CEm-a + Ib	✓
319/2017	IIA	RS	Bowl	H4(15) A1435 rP2	CEm-a + Ib	
320/2017	IIA	RS	Bowl	H4(15) A1435 rP2	CEm-a + Ib	✓
321/2017	IIA	RS	Bowl	H4(15) A1435 rP2	CEm-a + Ib	
322/2017	IIA	CP	Jar	H4(16) A1431 2b	CIb	

Table 1 (continued)

Sample	Phase	Ware classes	Description of the forms	Context	Petro group	XRFWDS
323/2017	IIA	CP	Jar	H4(12) A1432 rP2	VC1b	
324/2017	IIA	CP	Jar	H4(12) A1432 rP2	C1b	✓
325/2017	IIA	CP	Jar	H5(4) 2a	VCMgne + metag + Ib	

Each petrographic group is mentioned according to the following acronyms: V=vegeal tempered; C=calcareous matrix; E, M, and I=inclusions of effusive, metamorphic, and intrusive origin; b, m, a=basic, intermediate, and acid composition; for the metamorphic rocks, gne, metag, metaub, serp, and sc are abbreviations of gneisses, metagabbros, metapiroxenites, serpentinites, and schists; NC not classified

whole Upper Euphrates region, and Arslantepe gradually assumed the role of a frontier site at the margin of the empire (de Martino 2012).

Period VB (Late Bronze Age 1: VB1 = ca. 1700–1600 BC / VB2 = ca. 1600–1400 BC) is characterized by the presence of an impressive rampart that surrounded the entire mound (Palmieri 1978a: 35–37; Manuelli 2013: 41–43; Alvaro 2012: 350–352). The fortification was connected with a gate system flanked by protruding towers and enclosed a series of dwellings arranged for domestic good storage (Palmieri 1973: 58–71; Frangipane and Palmieri 1983: 289–290; Manuelli 2013: 48–66). Period IV (Late Bronze Age 2, ca. 1400–1250 BC) presents some interesting changes. The southern part of the site was gradually abandoned, and a new fortification system associated with a chambered gateway was built (Pecorella 1975: 3–5; Alvaro 2012: 353–355; Manuelli 2013: 404–409).

The downfall of the Hittite civilization represented the push factor for the emergence of a series of independent powerful reigns (Osborne 2021). The kingdom of Malizi/Melid had its capital at Arslantepe and its domain extended over a vast area westwards of the site up to the Euphrates river (Hawkins 2000: 282–329).

Period IIIA (Late Bronze-Iron Age transition: IIIA.1 = 1250–1200 BC / Early Iron Age 1: IIIA.2 = ca. 1200–1000 BC) is characterized by the presence of structures that directly overlap the destruction of the early gateway. A massive fortification wall keeps on enclosing the northern portion of the mound (Manuelli and Mori 2016). Period IIIB (Early Iron Age 2, ca. 1000–850 BC) in contrast marks an interesting change in the occupation pattern of the site. The former fortification wall was reused after its destruction, but associated structures are now exclusively represented by pits and silos and the entire area was devoted to grain storage (Frangipane et al. 2020: 81–86). Period IIA (Middle Iron Age, ca. 850–700 BC) shows a succession of three monumental-pillared halls built on top of the silos level. The building

sequence finds a direct stratigraphic connection with the structures belonging to the abovementioned “Lions Gate” (Liverani 2010).

The pottery repertoire

Because of the long history of investigations and the dissimilarities of the excavated contexts as well as the wide chronological framework, the Late Bronze and Iron Age pottery production at Arslantepe has been studied through many approaches and with different aims. The Late Bronze Age repertoire has been comprehensively examined and ultimately published (Manuelli 2013), while the Early Iron Age material has already been fully processed but its study is still ongoing (Manuelli 2018). On the other hand, the Middle Iron Age pottery assemblage has been only given a preliminary analysis, considering a restricted amount of better-preserved shapes and the most renowned ware classes (Frangipane et al. 2020: 92–98). This heterogeneity of the analyses has of course implied differences in the way the single wares have been processed, identified, and labeled (Table 1).

The Late Bronze Age and Early Iron Age wares have been macroscopically identified thanks to the co-occurrence of their main attributes, including pastes composition (mineral, vegetal, mixed), inclusions texture (coarse, semi-coarse, medium, semi-fine, fine, extremely-fine), surface treatments, colors of pastes and surfaces, decorations, manufacturing technologies, firing characteristics, and associations with specific shapes and their functional attributes (Manuelli 2013, 2018; Frangipane et al. 2020). In contrast, the Middle Iron Age wares have been macroscopically defined exclusively because of their cross-cultural correspondence with well-known coeval productions, and their classification is mostly based on the presence of specific decorative elements or surface treatments.



Fig. 2 Late Bronze Age ceramic wares groups: **a** Ware group A; **b** Ware group B; **c** Ware group C; **d** Ware group D; **e** Ware group E; **f** Ware group F (Red Lustrous Wheel-made Ware) (photos ©MAIAO)

The Late Bronze Age (Fig. 2)

The Late Bronze Age (ca. 1700–1250 BC) pottery production is characterized by 11 ceramic classes (Manuelli 2013: 82–89): mineral fabric and medium texture kitchen ware (A1), mineral fabric and coarse texture kitchen ware (A2), vegetable fabric and medium texture storage ware (B1), mineral-gritty fabric and medium texture common ware (C1), mineral-gritty fabric and medium texture orange common ware (C2), mineral-gritty fabric and semi-coarse texture common ware (C3), mineral-sandy fabric and fine texture ware (D1), mineral-sandy fabric and semi-fine texture ware (D2), mixed fabric and semi-coarse texture storage ware (E1), mixed fabric and coarse texture storage ware (E2), and mineral fabric and extremely-fine texture red ware (F1). The production is in general wheel-made and fired at well-controlled atmospheres. Pale color clays are mostly used, and surfaces are mainly characterized by a light and hasty smoothing. Decorations are rather common: painting with geometric patterns, red-decorative slips, and irregular drip marks have been identified on many of the abovementioned

wares (Manuelli 2022; Fragnoli and Rodler 2022). In general, the shape assemblage is characterized by the presence of elements that originate from the local Bronze Age tradition and the appearance of aspects related to the Hittite central Anatolian repertoire of the fourteenth and thirteenth century BC. A few more words should be said about Ware F: this is comparable to the so-called Red Lustrous Wheel-made Ware, a well-known and widely studied production mostly attested in northern Cyprus as well as southern and central Anatolia between the fifteenth and the thirteenth century BC (Mielke 2007; Kibaroglu et al. 2019).

The Early Iron Age (Fig. 3)

The Early Iron Age (ca. 1250–850 BC) pottery production is characterized by 8 ceramic classes (Manuelli 2018): mineral fabric and medium texture kitchen ware (K1), mixed fabric and coarse texture kitchen ware (K2), mineral fabric and semi-coarse texture storage ware (P1), vegetable fabric and coarse texture storage ware (P2), vegetable fabric and medium texture common ware (S1), mineral fabric and



Fig. 3 Early Iron Age ceramic wares groups: **a** Ware group K; **b** Ware group P; **c** Ware group S; **d** Ware group F (photos ©MAIAO)

semi-fine texture common ware (S2), mineral fabric and semi-coarse texture common ware (S3), and mineral fabric and fine texture ware (F1). The production is in general still characterized by the use of pale color clays, but firing must have now often taken place in a not very well-controlled atmosphere. Moreover, despite the fact that wheel marks are visible on nearly every sherd, it is possible that at least part of the production was only wheel-finished. Surfaces are exclusively poorly smoothed or self-slipped, decorations are virtually absent, and the assemblage is in general characterized by the total lack of any supra-regional ware. The Early Iron Age pottery shapes show on the one hand an interesting continuity of the Late Bronze Age tradition and on the other hand the introduction of new aspects typical of northern Syrian and the Levantine regions (Manuelli 2020: 118–121).

The Middle Iron Age (Fig. 4)

The Middle Iron Age (ca. 850–700 BC) repertoire is composed of 7 exogenous productions (Frangipane et al. 2020: 92–98). Red Slip Ware (RS) consists of mineral fabric, semi-fine texture, and orange color paste with a surface characterized by a red/orange layer accurately burnished. It is considered one of the hallmarks of the Levantine region from the ninth to the seventh century BC (Soldi 2013). Grooved Ware (GW) is a mixed fabric, semi-coarse texture, and gray color paste production with a set of grooved lines deeply incised. It is typical of the Iron Age in eastern Anatolia that appears along the western side of the Euphrates from the ninth century BC (Blaylock 2016: 15–20). Incised Ware (IN) shows mineral fabric, medium texture, and buff



Fig. 4 Middle Iron Age exogeneous ceramic wares: **a** Ware RS (Red Slip Ware); Ware GW (Grooved Ware); **c** Ware IN (Incised Ware); **d** Ware RB (Red Burnished Ware); **e** Ware AL (Alişar IV Ware) and Ware AB (Bichrome Alişar IV Ware); **f** Ware CP (Cypro-Phoenician Ware)

color paste with oblique or crossed lines incised on top of a red-slipped band. Again, in the Upper Euphrates region, it is mainly attested in the Middle Iron Age (Ökse 1988: 105–108). Red Burnished Ware (RB) consists of mineral fabric, semi-fine texture, and buff color paste with surfaces covered by a bright glossy red burnished slip. It is typical of the Urartian settlements in eastern Anatolia and found all the way to the Euphrates river (Batmaz 2020). Alişar IV Ware (AL) presents mineral fabric, medium texture, pale color paste, and a brown linear painted decoration applied over a thick white slip. Bichrome examples of Alişar IV Ware (AB) have mineral fabrics, semi-fine textures, and pale color pastes with white slipped surfaces and red and black-brown geometric paints. Alişar wares are typical of the Middle Iron Age in south-central Anatolia (d'Alfonso et al. 2022). Cypro-Phoenician Ware (CP) shows mineral fabric, semi-fine texture, pale color paste, and white slipped surfaces decorated with black-brown and/or red linear painted motifs. It suggests affinities with the so-called White Painted and Bichrome wares attested in the Cypro-Phoenician world from approximately the mid-ninth century BC (Gilboa 2015).

The geological setting

Arslantepe (Fig. 5) rests upon sediments from the Miocene era that were deposited in a lake setting and primarily comprise calcareous clays, sandstones, and limestones (Palmieri AM 1978b). Less than 1 km to the northeast, we find the Orduzu volcanics of the Middle Miocene with quartz-micromonzonites, basaltic trachyandesites, trachyandesites, and rhyolites (Önal 2008; Önal et al. 2008). The Baskil magmatics (Late Cretaceous) and the Yüksekova/Elazığ units (Maastrichtian to Early Eocene) crop out 5 to 6 km eastward. This area is dominated by a variety of intrusive and volcanic rocks, such as rhyolites, dacites, andesites, basaltic andesites, monzonites, tonalites, diorites, and gabbros (Yazgan and Mason 1988; Yiğitbaş and Yılmaz 1996). The extensive formations of the Anti-Taurus emerge 7 to 10 km south of Arslantepe. The Malatya metamorphics (Carboniferous-Triassic) occupy the western part of these units with meta-cherts, meta-clastic rocks, slates, phyllites, mica schists, and meta-carbonate rocks (Bozkaya et al. 2007; Robertson et al. 2006). The dominant features in the eastern portion consist of the Ispendere ophiolites (Late Cretaceous) and

the Maden Complex (Middle Eocene). The former showcases an undisturbed sequence of ophiolites that have been intruded by granites (Parlak et al. 2012), whereas the latter represents a volcano-sedimentary sequence encompassing andesites, altered basalts, cherts, radiolarites, spilitic lavas, mudstones, limestones, sandstones, and conglomerates (Şaşmaz et al 2014).

Materials and methods

The analysis has mostly taken into account ceramic vessels belonging to the Late Bronze Age ($n=36$) and Early to Middle Iron Age ($n=45+18$) in order to inspect elements of continuity and discontinuity between the two periods (Table 1). Sampling has been done to cover all the ware classes identified macroscopically, using a strategy that aimed to balance the number of samples per wares or, if not possible, per main group of wares according to their recurrence, availability, and possibility of sampling. The samples were analyzed through thin-section petrography ($n=96$) and XRFWDS geochemistry ($n=24$). As in previous papers, the emphasis has been put on thin-section petrography as more indicative of raw material procurement and processing due to both the predominance of coarse fabrics and the variety of the local geology (Fagnoli and Palmieri 2017; Fagnoli 2018). On the other hand, geochemical analyses have been more consistently performed on samples dating to the Middle Iron Age, considering the presence of exogenous productions in this period and the necessity to determine ceramic provenience and potential imports. In order to avoid biases related to the general limited number of samples, especially those analyzed geochemically, the data from the previous chronological phases have been considered in the study for comparison (Fagnoli and Palmieri 2017; Fagnoli 2018, 2019a, 2019b; Fagnoli and Liberotti 2019).

Thin sections were examined under the polarizing microscope LEICA DM 2700P and grouped according to textural, mineralogical, and technological features. Comparative charts were utilized to quantify the main components (Rice 1987: 348). Geochemical analyses were conducted with the wavelength dispersive X-Ray fluorescence spectrometer PANalytical AXIOS of the Archea Laboratory in Warsaw. Samples were treated with a corundum polishing machine to remove any contaminated surfaces, washed using distilled water and ultrasounds, and subsequently stored in a drying oven for 24 h before being transferred to a desiccator. Subsequently, the samples were ground using an agate mill (Fritsch Pulverisette Null) and left to dry once more. Afterward, a quantity of 1.5–2 g of powder was taken from each sample and subjected to

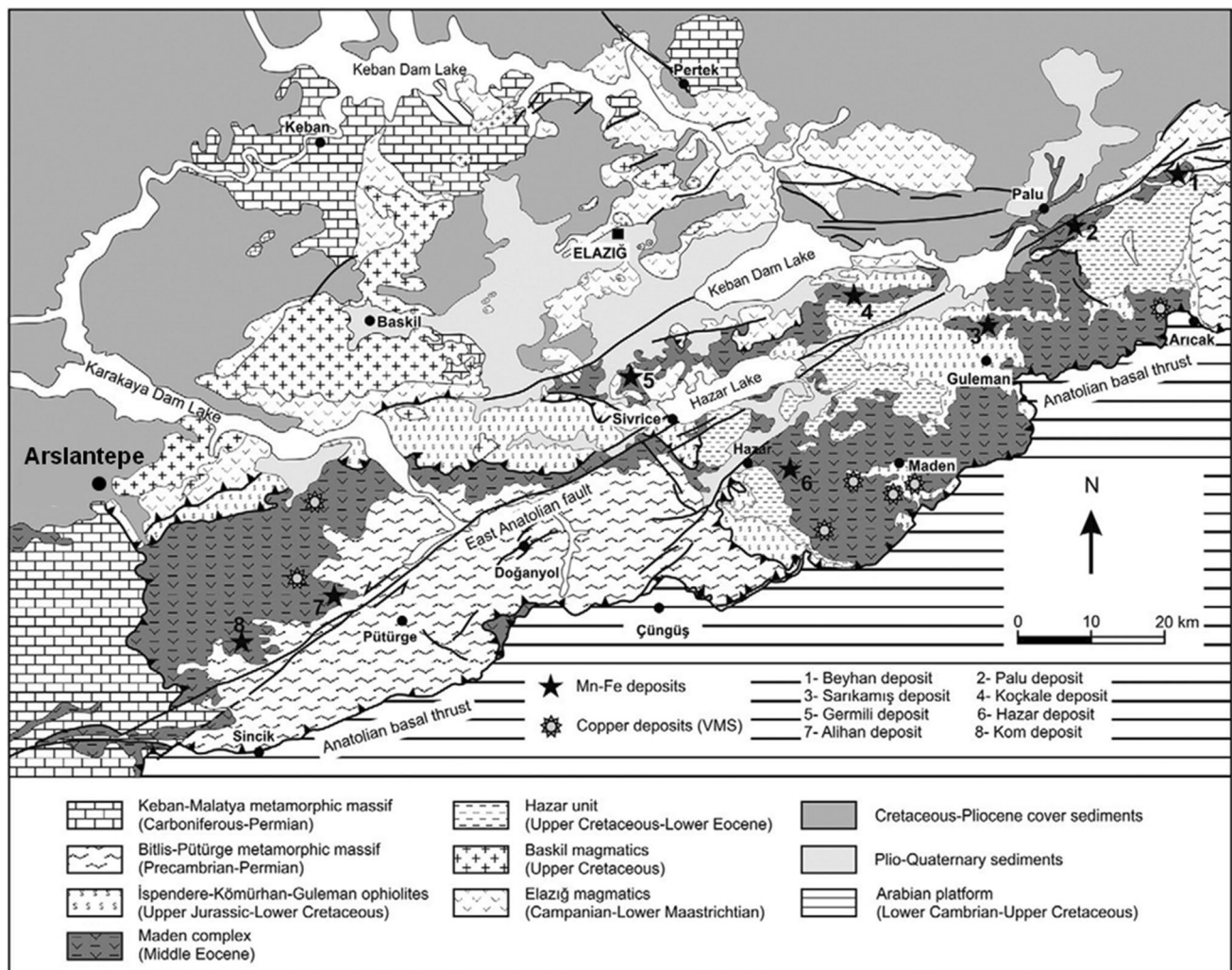


Fig. 5 Geological map of the Malatya-Elazığ region with indicated location of Arslantepe (based on the Turkish Geology Map by MTA (2002) at scale of 1:500,000)

ignition at 900 °C. The resultant material was then melted using a lithium-borate mixture (Merck Spectromelt A12) and cast into small discs measuring 32 mm in diameter. The concentrations of all major elements and of 14 trace elements were determined.

Thin-section petrography

The analyzed samples were classified into 16 petrographic groups based on several criteria, including the presence or absence of vegetal temper, the nature of the clay matrix (low- or high-calcareous content), and the geological origin of inclusions (Fig. 6, Table 1). Table 2 reports the detailed mineralogical and textural features of each group, named according to an acronym that indicates the predominant

components as explained in the caption of the table. Most of the samples (89.6%) exhibit a high-calcareous matrix, while about half of them (44.8%) are vegetal tempered. The shape of voids left by the burned-out vegetal temper is generally not assignable to agricultural by-products, such as spikelets, glumes, caryopses, or straw. Mineral and rock inclusions are predominantly of intrusive (62.5%) and to a lesser degree of volcanic (36.5%) and metamorphic origin (32.3%). Intrusive and volcanic rocks range from basic to acidic, while metamorphic rocks refer to either ocean-floor or low to high-grade regional metamorphism. Sedimentary rocks, such as sandstones, mudstones, and limestones, appear only in a negligible number of samples. The textural features are quite variegated as well, with maximum grain sizes and incidences between 0.3 and 7 mm and 7 and 30% respectively. Most of the ceramic pastes were tempered, as

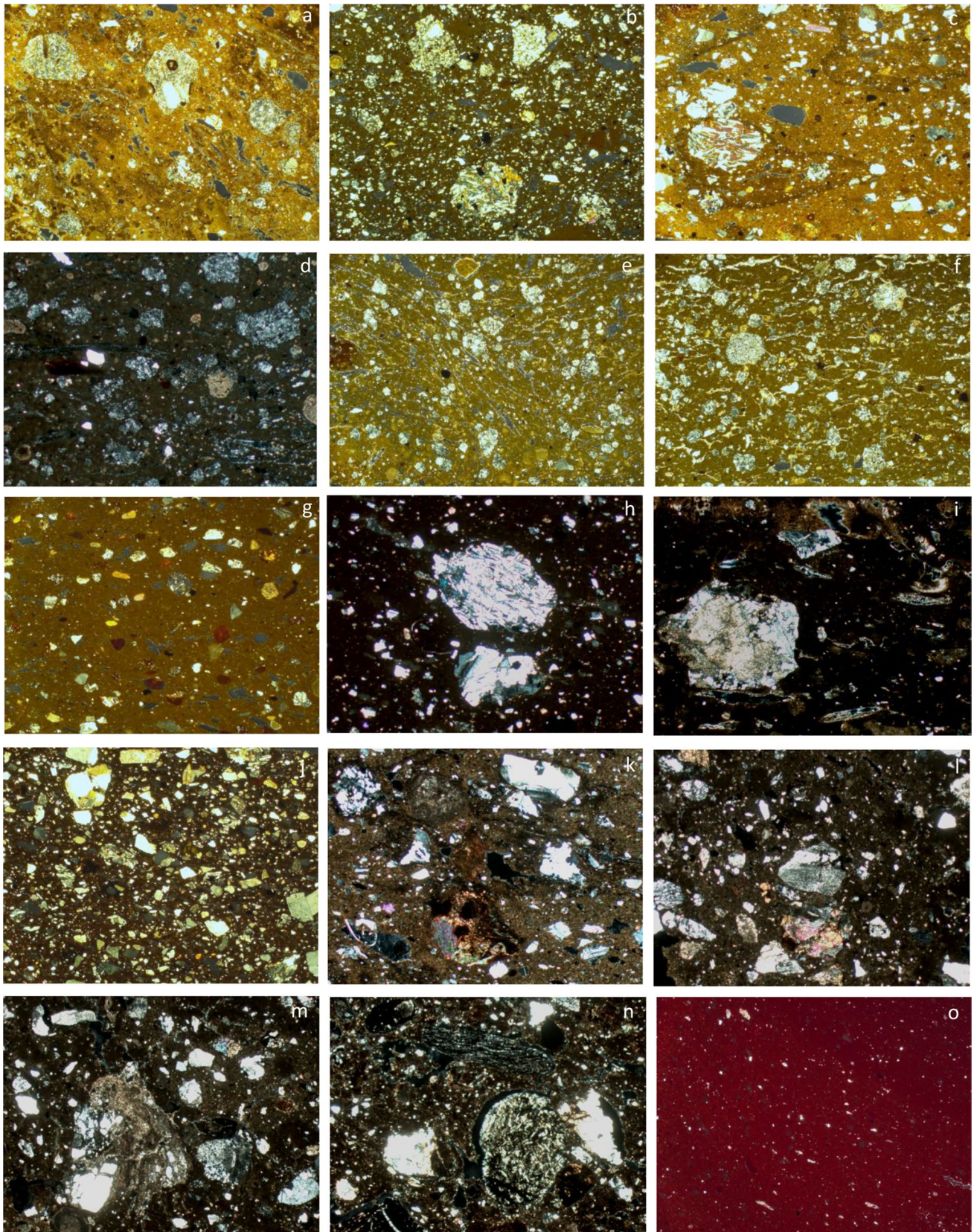


Fig. 6 Thin-section microphotographs under XP of petro groups: **a** VCEm-a+Ib; **b** CEM-a+Ib; **c** Clb; **d** VCEm-a; **e** VCEa; **f** CEa; **g** CEB-m; **h** Cl a+Ib; **i** VCla; **j** Ia+Ib; **k** VCMgne+metag+Ib; **l** and **m** CMgne+metag+metaub; **n** Mgne+serp+metag+sc; **o** Q. Field of view=6.85 mm (a; b; c; e; f; g; l; and o) and 4.8 mm (d; h; m; and n)

Table 2 Inclusions, clay matrixes and pores of the petrographic groups related to the Late Bronze to Middle Iron Age vessels from Arslantepe

PETRO. GR	Inclusions		Clay matrix				Porosity	
	Type	%	Shape	Grain-size distr	Max. Diam	Orientation		Birefringence
VCEm-a + Ib	veg, ca, trachytes-rhyolites, gabbros, pl, qu, limestones, horn, ox, sandstones, cpx, for, bt, opx, mu, ol	25–30	ang-subround	polymod	6.4	Random-moderately	Inactive-active	Equidimensional, elongated, random, and parallel
CEm-a + Ib	ca, trachytes-rhyolites, gabbros, pl, qu, limestones, horn, ox, sandstones, cpx, for, bt, opx, mu, ol	10	subang-subround	bimod.-polimod	2.8	Random-moderately	Sintered-active	Elongated, equidimensional, random
VCIb	veg, ca, gabbros, pl, ox, cpx, trachytes-rhyolites, qu, opx, limestones, for, horn, bt, mu	20–25	ang-subang	polymod	5.04	Random-strongly	Slightly active-active	Equidimensional, elongate, random
CIb	ca, pl, ox, qu, bt, cpx	7–10	subang-subround	bimod	2.2	Random-moderately	Sintered-active	Equidimensional, random
VCEm-a	veg, ca, trachytes-rhyolites, limestones, qu, pl, ox, horn, bt, mu, sandst., for, cpx, ep, kfds, qu-schists qu, opx, gabbros	20–25	subang-subround	polymod	3.6	Random-moderately	Sintered-inactive	Elongated, random, and parallel
CEm-a	ca, trachytes-rhyolites, limestones, pl, ox, mu, horn, bt, gabbros, for, opx, pumices, qu-schists	10–15	subang-subround	polymod	2.8	Moderately	sintered-slightly active	Equidimensional, random
VCEa	veg, rhyolites-dacites, pl, qu, bt, gabbros, ox, horn, cpx	15	subround	bimod.-polymod	2.4	Random	Inactive-slightly active	Equidimensional, elongate, random
CEa	rhyolites-dacites, pl, qu, bt, ox, horn, cpx, veg, gabbros, for, sandstones, mu	10–15	subround-subang	polymod	2.8	Random	Inactive-slightly active	Equidimensional, random
CEB-m	ca, pl, qu, basaltic andesites, bt, granoblastic qu-fds aggregates, horn, cpx, ox, mu, veg, for, kfds, qu-schists qu, ep	7–15	subround-subang	uni-bimod	0.8	Random-strongly	Sintered-slightly active	Elongated, parallel
CIa + Ib	ca, granites, gabbros, qu, pl, kfds, ox, horn, bt, ep, veg, sandstones	15–20	subang-ang	polymod	6	Slightly-strongly	Sintered-slightly active	Equidimensional, elongated, random and parallel

Table 2 (continued)

PETRO. GR	Inclusions		Clay matrix				Porosity	
	Type	%	Shape	Grain-size distr	Max. Diam	Orientation		Birefringence
VCla	veg, ca, granites, qu, kfds, pl, limestones, sandstones, cpx, ox, trachytes-rhyolites, for, horn, bt, chert	15	subarr-subang	polymod	7	Random-moderately	Sintered-slightly active	Equidimensional, elongated, random
Ia + Ib	granites, qu, gabbros, pl, kfds, horn, ox, cpx, bt, ep, sandstones veg	15–20	subang	polymod	2.4	Random-slightly	Inactive-moderately active	equidimensional, elongated, parallel
VCMgne + metag + Ib	metagabbros, gneisses, ca, gabbros, veg, pl, qu, kfds, for, cpx, ep	20–30	ang-subang	polymod	4.1	Random	Slightly active-active	Equidimensional, elongated, parallel
CMgne + metag + metab	gneisses, ca, qu, ox, kfds, cpx, pl, bt, for, horn, metapyroxenites, metagabbros, limestones, ep, epidotes	10–15	subang-ang	bimod.-polymod	2.9	Random	Sintered-slightly active	Equidimensional, elongated, parallel
Mgne + serp + metag + sc	gneisses, serpentinites, metagbbros, qu-schists, pl, qu, ca, limestones, limestones, metabasalts, graph-schists, mu-schists, horn, for, rhyolites, mudstones, marbles, cpx, bt	20–25	subang-ang	polymod	4.2	Random	Inactive-slightly active	Equidimensional, elongated, random
Q	qu, ox, mu, horn	7	subround-subang	unimod.-bimod	0.3	Random	Inactive-moderately active	Equidimensional, elongated, random

Each petrographic group is mentioned according to the following acronyms: V = vegeral tempered; C = calcareous matrix; E, M, and I = inclusions of effusive, metamorphic, and intrusive origin; b, m, a = basic, intermediate, and acid composition; for the metamorphic rocks, gne, metag, metab, serp, and sc are abbreviations of gneisses, metagabbros, metapyroxenites, serpentinites, and schists; Q = dominated by quartz grains. The types of inclusions are listed in decreasing order of frequency and are italicized in case they are not present in each sample. Abbreviations: veg vegetal matter, ca calcite; pl plagioclases; qu quartz, horn hornblendes, ox oxides, cpx clinopyroxenes, for foraminifera, bt biotites, opx orthopyroxenes, mu muscovites, ol olivines, ep epidotes, kfds K-feldspars

Table 3 Seriation table of petro groups and summarizing table (below) evidencing continuity and changes between the Late Bronze and Iron Age

	VCEa	CEa	CEm-a	VCEm-a	Mgne+serp+metag+sc	Q	Cib	CEa-m+Ib	CEb-m	Ia+Ib	VCEa-m+Ib	Cla+Ib	CMgne+metag+metaub	VCIa	VCib	VCMgne+metag+Ib
LBA1A	1	1	1	2			2	1								
LBA1B		1	1	1		1				3	1					
LBA2			1	2		2	3			4		1				
EIA							2	3		2	3	5		4	6	1
MIA							4	5	1		2				3	
TOT							17				34					36

LBA-EIA	%
Disappearance	20
Continuity	39
Novelty	41

Petrographic groups are mentioned according to the following acronyms: V = vegetal tempered; C = calcareous matrix; E, M, and I = inclusions of effusive, metamorphic, and intrusive origin; b, m, a = basic, intermediate, and acid composition; for the metamorphic rocks, gne, metag, metaub, serp, and sc are abbreviations of gneisses, metagabbros, metaproxenites, serpentinites, and schists; Q = dominated by quartz grains

demonstrated by the polymodal grain sizes, clustered distribution, and angular shapes of inclusions.

As in the prehistoric phases, the Late Bronze and Iron Age assemblage from Arslantepe displays a wide textural and geological variety (Fragnoili and Palmieri 2017). Among the large spectrum of recipes, 9 out of 17 (46%) were already used in the Late Chalcolithic and Early Bronze Age phases¹. Most of them—i.e., petro groups CEa + Ib, CEm-a, Cib, VCEa-m + Ib, VCEm-a, and VCib—typically occur in the light-colored wheel-finished vessels dating to the Late Chalcolithic 3 to 5 (periods VII and VIA of the site sequence). Clay matrixes are calcareous and tempered with trachytic lavas and/or microgabbros from the Baskil and Yüksekova complexes available 6 to 15 km east of the site. Both vegetal-tempered and non-vegetal-tempered variants exist. Two other calcareous recipes, both tempered with rhyolitic lavas from the Orduzu suite (900 m east from the site) but differing in the use or non-use of vegetal temper (VCEa and CEa), first appeared in the Early Bronze Age 1 Handmade Red-Black Burnished Ware (Periods VIB1-2). One last calcareous recipe distinguished by basaltic andesites and altered clinopyroxenes typically occurs in the Early Bronze Age 2 and 3 (Periods VIC-D) handmade painted vessels.

Forty-one out of 96 samples show recipes that are not attested in the previous phases of the site sequence (Table 1). Most of these (i.e., 24 samples) exhibit a large variety of metamorphic rocks, such as gneisses, serpentinites, metagabbros, metaproxenites, metabasalts, and quartz- and mica schists. These lithologies are available 7 to 10 km south and southeast of the site within the Ispendere ophiolites, Maden Complex, and Malatya metamorphics. Three distinct recipes—i.e., VCMgne + metag + Ib; CMgne + metag + metaub;

and Mgne + serp + metag + sc—were identified based on the incidence of each type of rock, the presence of vegetal temper, and the high- vs. low-calcareous nature of the clay matrix. Fourteen other samples are made of three recipes—i.e., VCIa, CIa + Ib, and Ia + Ib—that share granitic rocks as the main lithic inclusion, but differ in the presence or absence of microgabbros and vegetal temper as well as in the calcareous nature of the matrix. A procurement from the eastern Baskil and Yüksekova complexes, which also exhibits intermediate to sialic intrusive rocks besides gabbros and trachytic lavas, is assumable. Three samples exhibit a fine-grained coral-red recipe (i.e., Q) almost totally dominated by quartz inclusions, which are not diagnostic in terms of provenance.

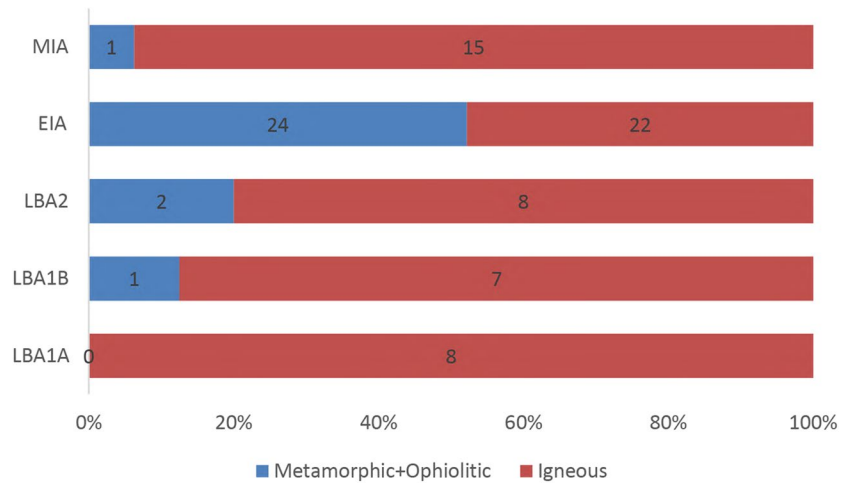
Discussion of the petrographic results

The distribution of samples into petro groups (Table 3) evidences elements of both continuity and change between the Late Bronze and Iron Age. Thirty-nine percent of the samples share recipes—i.e., CEb-m, VCEa-m + Ib, CEa-m + Ib, Cib, and Ia + Ib—that invariably occur in both periods. At the same time, the Iron Age marks the disappearance and appearance of old and new recipes in respectively 20% and 41% of the samples. One new recipe (petro group VCMgne + metag + Ib) now clearly predominates over both the new and older ones. In general, the Early Iron Age represents a break in the strategies of raw material procurement, with respect to both the previous and subsequent phases. Indeed, the eastern igneous deposits are mostly exploited across all the phases except during the Early Iron Age, which shows a gravitation towards the southern metamorphic and ophiolitic deposits (Fig. 7).

Interesting trends emerge when considering the Late Bronze Age and Iron Age separately in relation to the respective repertoire of wares and/or shapes. In the Late Bronze Age, the same wares are produced with different

¹ Though sharing the same minero-petrographic associations, some pastes are finer in the prehistoric phases, i.e., present a lower amount of smaller inclusions.

Fig. 7 Exploitation of southern metamorphic and ophiolitic sources vs. exploitation of eastern igneous sources from the Late Bronze to the Middle Iron Age



recipes, and conversely, the same recipes occur in different wares. The only exceptions are the Red Lustrous Wheel-made Ware F1 as well as the painted examples of the semi-fine D2 and storage E1/E2 wares, which are realized with specific recipes. The recipes recurring in the painted wares—i.e., CEm-a, CEb-m, and VCEm-a—date back to the prehistoric tradition, while the Red Lustrous Wheel-made Ware is made of a peculiar recipe, namely the abovementioned petro group Q. This latter fits with the fine fabric group reported for most of the Red Lustrous wares found across the eastern Mediterranean and interpreted as a Cilician production based on the latest archeological and archaeometric evidence (Kibaroglu et al. 2019). Most of the petro-loners (Fig. 8) present the same intrusive and metamorphic local lithotypes as those mentioned above, but differently combined (Table 4). The only exception is the flat bowl 347/15 (Fig. 8g), distinguished by peculiar minero-petrographic associations not observed in other samples yet, i.e., calcareous sandstones and intrusive intermediate rocks.

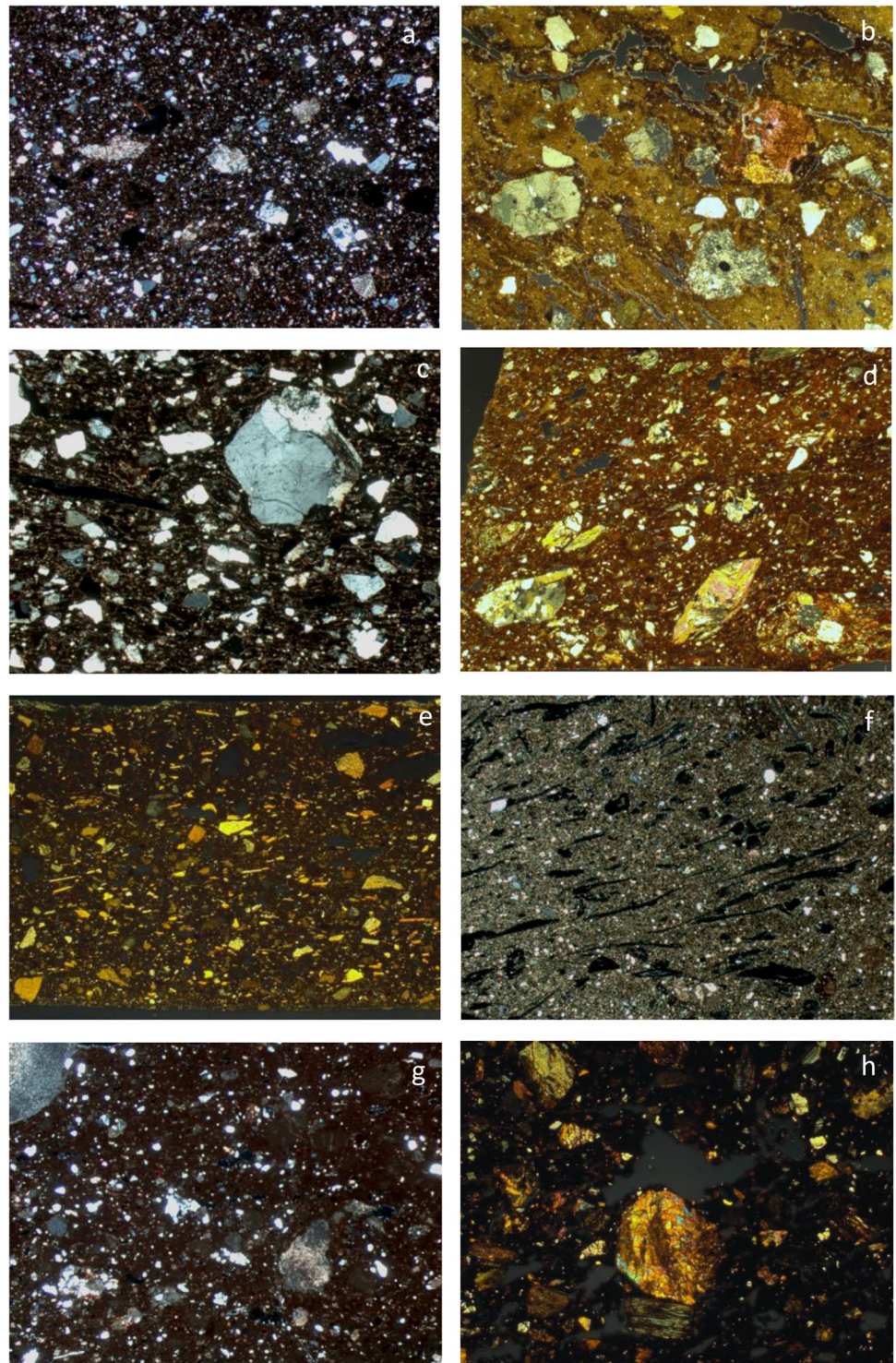
By the Early Iron Age, cooking pots started being produced with standardized paste preparation modes, as indicated by the predominance of petro group VCMgne + metag + Ib, while other shapes still exhibit variegated recipes. During the subsequent Middle Iron Age, the decorated wares of the allochthonous tradition—such as the Cypro-Phoenician and Alişar IV painted wares as well as the Syrian Red Slip and Urartian Red Burnished wares—are mostly locally produced with recipes that are well-documented along the previous site sequence (petro groups CIb, VCEm-a + Ib, Ib, CEm-a + Ib, and CEb-m). In particular, specific recipes recur, on the one hand, in the Urartian and Cypro-Phoenician wares (petro groups VCIB and CIb) and, on the other hand, in the Red Slip Ware (petro group CEm-a + Ib). However, the only Grooved Ware carinated bowl here analyzed (sample 350/15) and 1 of the bichrome Alişar IV Ware jars (sample 355/15) could

not be classified into any groups, which likely reflects a foreign origin (Table 4). Both samples are non-calcareous with a medium-coarse texture; the Alişar IV Ware jar is dominated by clinopyroxenes and altered mafic minerals (Fig. 8e), while the Grooved Ware carinated bowl is rich in metapyroxenites, vegetal temper, and clinopyroxenes with exsolution and replacement textures (Fig. 8). The minero-petrographic association of both samples indicates the ophiolitic nature of the supply sources. Similar sources are widely reported in Turkey, especially along the Ankara-Erzincan and Bitlis-Zagros suture zones (Fig. 9). Considering the regions where these 2 ware classes are mostly produced and spread, a general link with the Ankara-Erzincan zone could be assumed. Locally produced and imported Alişar IV Ware vessels also differ by the surface treatments: the surfaces of the former do not exhibit any slipping layer, while those of the latter are covered by a thick regular and calcareous slip (Fig. 10).

XRFWDS geochemistry and comparison with petrography

Upon relating the various chemical elements (Table 5) in binary plots, 3 distinct groups emerge (Fig. 11): the largest group includes both Late Bronze and Iron Age samples, while the 2 minor ones are each composed of only 3 samples mostly dating to the Late Bronze Age 1–2 phases. The first minor group includes a Late Bronze Age 1B-2 arm-shaped vessel (329/17), a Late Bronze Age 2 pedestal base (332/17), and a Late Bronze Age 2 high-necked small-sized bottle (336/17), all distinguished by higher Al_2O_3 , Fe_2O_3 , and Rb and minor MnO values. The sample 336/17 further differs by higher Zr and Rb contents. Unfortunately, thin sections could not be prepared from these samples due to material scarcity. The second minor group is comprised of a Late Bronze

Fig. 8 Thin-section microphotographs under XP of petrologers: **a** 241/15; **b** 325/15; **c** 331/15; **d** 306/15; **e** 355/15; **f** 342/15; **g** 347/15; **h** 350/15. Field of view = 6.85 mm (**b**; **d**; **e**; and **h**) and 4.80 mm (**a**; **c**; **f**; and **g**)



Age 2 neckless medium-sized cooking pot (327/15), a Late Bronze Age 1B short-necked medium-sized cooking pot (331/15), and an Early Iron Age flat bowl (305/17), which are richer in SiO_2 and poorer in CaO, Ba, Cr, and Sr. Although these 3 samples have different mineralogical associations, they all share the low-calcareous nature of the clay matrix and the presence of

felsic rocks (e.g., granites, gneisses, quartz-schists, trachytic to rhyolitic lavas). The sample 327/15 is further distinguished by higher Mn, V, and Ti values, which fit with the occurrence of ophiolitic rocks observed under the polarizing microscope.

By adding the data of locally produced samples from the previous phases, we notice that all the Late Bronze-Iron Age

Table 4 Inclusions, clay matrixes, and pores of the petrographic loners related to the Late Bronze to Middle Iron Age vessels from Arslantepe

Sample	Inclusions						Clay matrix	Porosity
	Type	%	Shape	Grain-size distr	Max. Diam	Orientation	Birefringence	Shape and orientation
241/15	ca, qu, marbles, gneisses, quartzites, mu, pl, ep, for, mu-schists	15	ang-subang	bimod	0.96	Random	Active-slightly active	Equidimensional, random
325/15	veg, trachytes-rhyolites, gneisses, qu, metagabbros, cpx, pl, limestones, for, kfds, horn	25	ang-subround	polymod	5.15	Weakly-moderately	Active-slightly active	Elongate, parallel
331/15	granites, qu, kfds, ox, bt, pl, veg, horn	20	ang-subang	bimod	2.1	Random	Active-slightly active	Elongate, parallel
306/15	qu-schists, mu, qu, mu-schists, pl	20	ang-subang	bimod	3.36	Moderately-random	Active-slightly active	Elongate, parallel
355/15	cpx, sandstones, kfds, qu	15–20	ang	bimod	1.76	Moderately-random	Slightly active	Equidimensional, random, parallel
342/15	veg, ca, qu, pl, mu, qu-schists	20–25	subang-ang	bimod	3.05	Random	Active	Equidimensional, random
347/15	sandstones, pl, ca, qu, gneisses, mu, kfds, qu-schists, norites, horn, ep	10–15	subround-subang	bimod	1.36	Random	Inactive-sintered	Equidimensional, random
350/15	veg, metapyroxenites, cpx, pl, metagabbros, mu, ep	15	ang-subang	polymod	1.3	Random	Inactive	Elongate, parallel, random

The types of inclusions are listed in decreasing order of importance. Abbreviations: *ca* calcite, *qu* quartz, *mu* muscovites, *pl* plagioclases, *ep* epidotes, *for* foraminifera, *kfds* K-feldspars, *veg* vegetal matter, *cpx* clinopyroxenes, *horn* hornblendes, *ox* oxides, *bt* biotites

samples, including those of the 2 minor groups, fall into a typical local range (Fig. 12). This also concerns the 2 minor groups that show chemical affinities with Late Chalcolithic 4 to Early Bronze Age 1 cooking and Red-Black Burnished Ware vessels generally realized with metamorphic raw materials.

To identify potential variations and similarities among the samples, a principal component analysis (PCA) was

conducted using the SPSS software package. Raw chemical values were adjusted to a constant sum of 100%, logarithmically transformed to base 10, and standardized to provide a roughly equal weight for all elements during calculation (Baxter 1994, 1995, 2003a, 2003b; Glascock 1992). CaO, Na₂O, and P₂O₅ were excluded from statistical analyses due to their susceptibility to post-depositional alterations (Free-stone et al. 1985; Schwedt et al. 2004). The same 3 groups

Fig. 9 Distribution of ophiolites in correspondence of the suture zones (Sarifikioğlu et al. 2014)

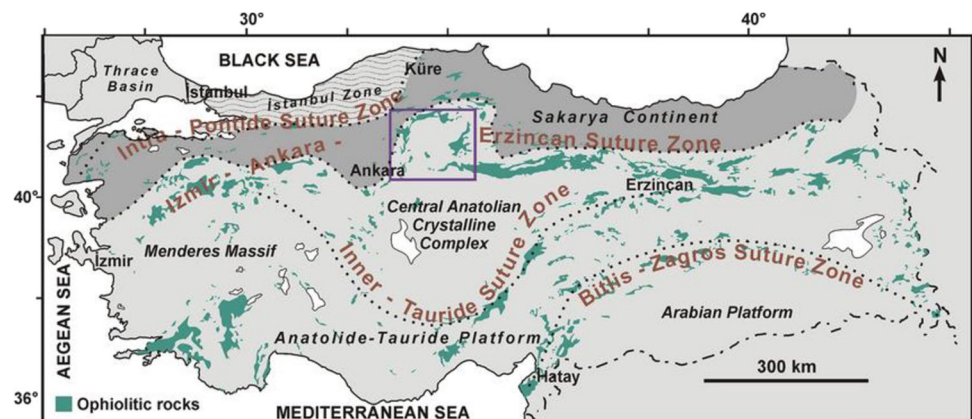
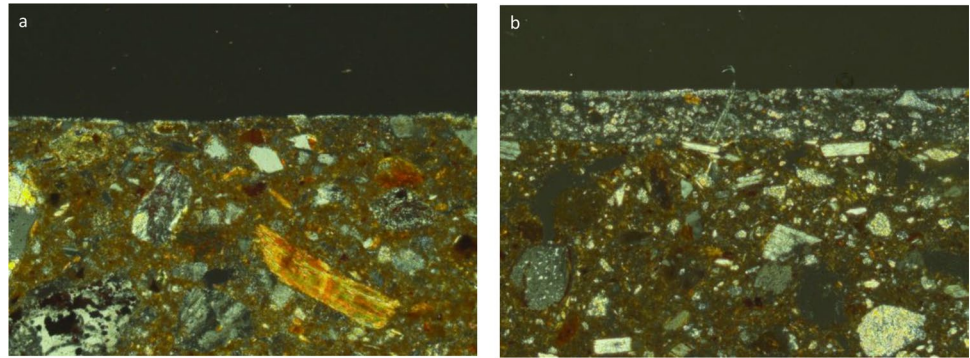


Fig. 10 Distinct surface treatments between locally produced (a) and imported (b) Alişar IV Ware sherds. Field of view: 0.9 mm



of samples mentioned above emerge in the PCA plot that relates the first and second factors (Fig. 13). These account for 66.6% of the total variance and consider Al_2O_3 , -Ni, Fe_2O_3 , MgO, SiO_2 , -Sr, -Cr, TiO_2 , V and - K_2O , Ba, MnO, Rb, respectively. Both the first and second minor groups differ from the rest of the samples by higher values of factor 1, which well reflect the presence in thin sections of both mafic and sialic rocks. As for factor 2, the first minor group is poorer, and the second richer. Within the largest group, which includes vessels of any wares, shapes, and periods, a subgroup of three samples now stands out due to lower values of factor 2. This subgroup only includes Late Bronze Age 1-2 necked pithos with drip marks, which do not show any distinct petrographic features compared to other samples though. This might presumably indicate the use of distinct local clay sources for this ceramic class.

Conclusions

The results obtained through thin-section petrography and XRFWDS geochemistry evidenced both elements of continuity and discontinuity between the Late Bronze and Iron Age. The elements of continuity concern the use of recipes made of volcanic raw materials available east of the site and already attested by the prehistoric phases. These recipes typically recur in the Late Bronze and Middle Iron Age painted productions, while unpainted vessels are distinguished by more variable and thus less specialized recipes. On a wider geographical perspective, it is interesting to note that this result contrasts with the evidence of the Late Bronze Age painted pottery from Oymaağaç Höyük/Nerik, Central Black Sea, which exhibits instead a large petrographic and geochemical variability (Mielke et al. 2021).

The most evident changes in the local production marked by the Iron Age consist in a much stronger gravitation towards the southern Anti-Taurus mountains for the procurement of raw materials, the appearance of new recipes in the common wares, the standardization of paste recipes for the

cooking pots and, more generally, a trend towards a compositional homogenization. In this framework of changes, it is important to stress once again that widespread transformations and the introduction of new sets of inter-cultural connections with regions located south of the Malatya area are also clearly visible in the shape repertoire of the pottery assemblage since the very beginning of the Iron Age. At the same time, a strong standardization in terms of the decrease in shape varieties and macroscopic identification of fabrics and wares characterizes the entire Early Iron Age collection when compared to the previous Late Bronze Age. It is nevertheless worth mentioning that the morphological standardization does not unequivocally correspond to more standardized recipes, for example, as in the case of the flat bowls that were produced with at least 5 different recipes. The evidence of cooking pots recalls instead a phenomenon that took place at different times in the whole eastern Mediterranean, namely the emergence of specialized cooking pottery centers (Ben-Shlomo 2019). This is often accompanied by changes in paste preparation and vessel shaping, although the role that food-related practices had on these changes or, conversely, the impact that these changes had on food-related practices still remain poorly investigated.

Further differences concern the incidence of imports in relation to foreign wares, following a pattern that mostly reflects what has been shown by the archeological evidence. During the Late Bronze Age, the only foreign ware is the Red Lustrous Wheel-made Ware, which is always imported from Cilicia. In the Early Iron Age, both foreign wares and imports are lacking. The Middle Iron Age is in contrast distinguished by several wares of foreign tradition, which are mostly locally produced. However, some nuances are still discernible within this general trend: while there are a few imports from south-central and eastern Anatolia (e.g., Alişar IV and Grooved wares), the wares of the southern tradition (e.g., Red Slip and Cypro-Phoenician wares) are exclusively locally made. This is a noteworthy aspect that might further emphasize the fact that contacts with the regions south of Malatya were well-established since the end of the Late Bronze Age, while eastwards and westwards these became

Table 5 Major (wt. %) and trace element (ppm) concentrations. Elements between brackets are under the detection limit

Sample	SiO ₂	TiO ₂	Al ₂ O ₃	Fe ₂ O ₃	MnO	MgO	CaO	Na ₂ O	K ₂ O	P ₂ O ₅	V	Cr	Ni	(Cu)	Zn	Rb	Sr	(Y)	Zr	(Nb)	Ba	(La)	(Ce)	(Pb)
329/2015	57.42	0.482	12.77	4.29	0.103	3.05	16.48	1.64	3.24	0.54	61	240	132	10	84	84	367	21	136	15	528	25	50	20
336/2015	44.61	0.596	10.01	5.50	0.091	5.90	28.79	0.84	3.28	0.38	108	490	262	17	81	49	445	21	110	14	277	8	31	8
342/2015	48.08	0.684	11.86	6.09	0.11	4.52	23.75	0.76	3.87	0.28	107	442	223	49	88	58	458	25	155	16	373	16	27	13
331/2015	65.96	0.730	17.35	7.86	0.126	2.05	1.71	1.93	2.21	0.07	172	116	61	43	68	35	92	33	121	9	152	6	8	5
338/2015	56.31	0.551	12.93	4.78	0.075	3.36	17.59	1.28	2.90	0.22	86	264	127	11	66	89	392	21	142	15	431	42	34	17
327/2015	57.67	1.211	18.60	10.74	0.234	3.32	4.95	1.37	1.79	0.12	195	273	133	43	101	51	226	32	147	11	202	11	29	9
339/2015	55.58	0.534	12.75	4.74	0.108	3.24	18.50	1.29	2.98	0.28	69	266	139	20	63	84	382	18	130	16	493	34	54	16
344/2015	47.77	0.609	11.57	7.14	0.114	8.37	20.06	1.47	2.46	0.45	108	500	366	54	93	44	367	12	65	16	544	/	/	11
309/2015	47.55	0.951	12.87	6.77	0.102	6.10	21.54	1.37	2.40	0.35	160	300	245	33	90	51	752	22	136	14	612	32	17	9
310/2015	52.57	0.715	13.74	7.07	0.120	6.32	15.45	1.23	2.51	0.26	149	286	241	29	98	68	704	23	129	14	340	15	52	11
313/2015	53.93	0.569	13.50	6.78	0.114	4.98	15.43	1.44	3.08	0.18	129	227	188	52	103	53	402	14	85	13	598	/	/	11
324/2015	50.39	0.672	13.15	6.65	0.112	5.69	19.21	1.24	2.67	0.22	152	272	229	36	80	58	701	21	126	13	327	30	36	9
325/2015	50.39	0.575	12.70	6.19	0.094	5.31	21.29	1.07	2.24	0.13	122	276	221	26	72	51	495	21	113	12	275	15	25	10
349/2015	56.66	0.975	15.29	6.56	0.104	5.10	9.66	2.32	3.08	0.25	104	216	210	32	88	74	525	21	146	16	450	7	21	13
352/2015	49.15	0.897	13.53	6.61	0.100	4.88	19.96	2.05	2.61	0.21	104	319	244	46	112	37	498	16	104	13	503	/	/	4
353/2015	49.12	1.012	12.98	6.30	0.093	5.01	20.91	2.07	2.24	0.27	133	403	199	43	76	51	565	19	150	15	326	18	26	9
354/2015	51.83	0.866	13.67	7.35	0.132	5.37	16.76	1.80	2.03	0.19	143	514	190	45	88	50	446	27	169	16	282	25	41	9
356/2015	48.62	0.672	11.47	6.30	0.098	7.41	21.13	1.21	2.87	0.21	121	455	361	33	95	57	585	16	114	12	266	<5	24	14
359/2015	49.71	0.906	13.53	6.67	0.096	5.60	18.04	2.10	3.09	0.25	101	259	238	51	99	42	458	14	102	16	524	/	6	13
301/2017	44.84	0.725	11.09	6.17	0.100	6.01	27.81	0.76	2.28	0.216	117	399	248	26	70	38	556	18	117	11	201	17	32	9
305/2017	63.68	0.936	17.69	7.77	0.122	2.33	3.55	2.26	1.54	0.119	157	125	54	28	83	53	190	31	146	13	180	10	35	9
311/2017	42.52	0.555	10.04	5.20	0.073	4.68	33.32	0.72	2.67	0.224	107	663	210	52	89	44	455	20	126	14	266	32	38	10
348/2017	49.68	0.584	11.24	7.09	0.102	8.13	19.11	1.30	2.49	0.270	125	495	394	43	105	54	551	18	111	13	178	12	35	8
320/2017	51.61	0.761	13.23	6.34	0.098	5.70	16.97	1.69	3.28	0.30	116	268	255	120	94	74	699	20	142	15	298	26	54	10
324/2017	47.98	0.878	13.27	6.72	0.101	5.50	20.28	1.90	3.13	0.23	99	298	231	180	104	37	538	17	94	13	279	/	16	/
329/2017	54.50	0.930	22.22	8.34	0.057	2.60	8.32	0.21	2.69	0.15	137	132	75	110	95	115	212	25	121	21	528	/	64	/
332/2017	53.78	0.904	21.18	8.66	0.061	3.08	8.82	0.25	3.11	0.15	132	130	77	70	106	125	273	22	122	21	458	/	48	/
336/2017	54.76	0.867	19.80	7.98	0.056	2.82	10.18	0.29	3.06	0.19	147	130	59	27	78	155	348	33	192	20	403	33	77	14
318/2017	52.41	0.822	13.68	6.51	0.097	5.50	15.47	1.75	3.53	0.23	98	230	245	168	108	44	399	18	76	15	269	/	<5	/
346/2017	52.94	0.628	13.06	7.05	0.126	6.86	15.17	1.23	2.61	0.32	112	365	277	94	104	46	264	14	60	13	307	/	46	/

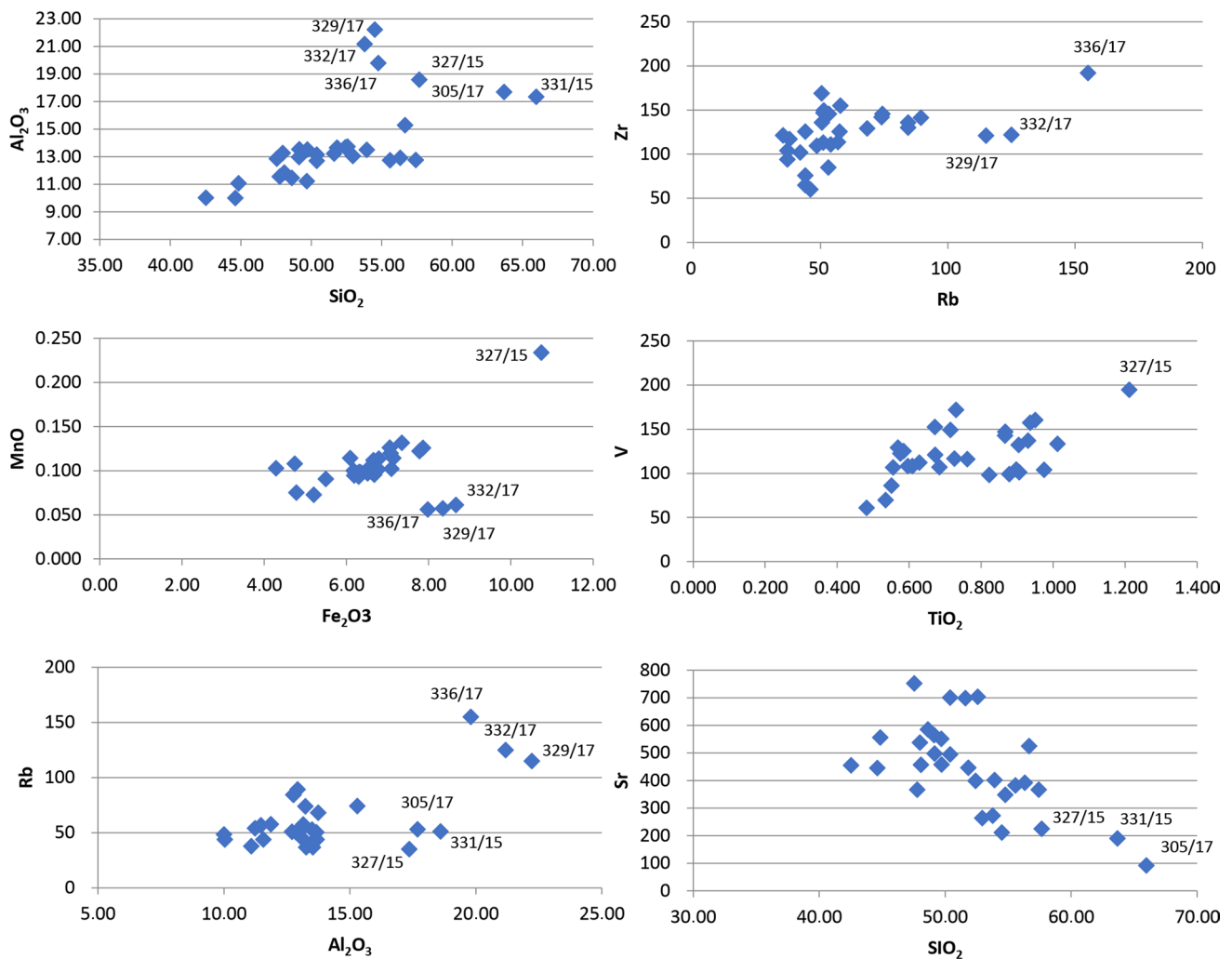


Fig. 11 Binary plots showing the distinct concentrations of some elements for the samples 329/17, 332/17, 336/17, 337/15, 331/15, and 305/17

more irregular and probably did not affect the local production pattern. At any rate, our analysis also demonstrates that Alişar IV Ware was not only the product of a few centers in south-central Anatolia (d'Alfonso et al. 2022) but could also be produced far away from this region. Moreover, as already documented at an intra-regional level (d'Alfonso et al. 2022), the analysis has further shown that Alişar IV Ware local imitations and imports differ by surface treatments and decoration also at Arslantepe.

The abovementioned changes could also be briefly considered within a wider socio-economic, cultural, and historical perspective. The occurrence of imported Red Lustrous Wheel-made Ware specimens in Late Bronze Age 2 contexts confirms the gradual involvement of Arslantepe in the mechanism of expansion of the Hittite empire and further highlights interesting connections between its peripheral regions. With the collapse of the Late Bronze Age centralized system and the emergence of the Early Iron Age regional

states, new trajectories of contacts and influences occur. Connections with regions located south of the Malatya area are manifested in both the procurement of raw material and the pottery repertoire. These are clearly related to the growing political and cultural role of Karkemiş during the last centuries of the second millennium BC. At the same time, the standardization of some paste recipes and shapes might imply the existence of a strong local power able to impose control over the means of pottery production. The Middle Iron Age shows instead the emergence of a new and vivid cultural environment, placing Arslantepe at the center of a renewed system of extra-regional exchange, as is shown by the presence of several wares belonging to foreign traditions. This trend reflects the multicultural nature of the Syro-Anatolian world at the beginning of the first millennium BC.

In conclusion, this study demonstrates the importance of raw material procurement and processing as indicators of socio-economic and cultural changes over the longue

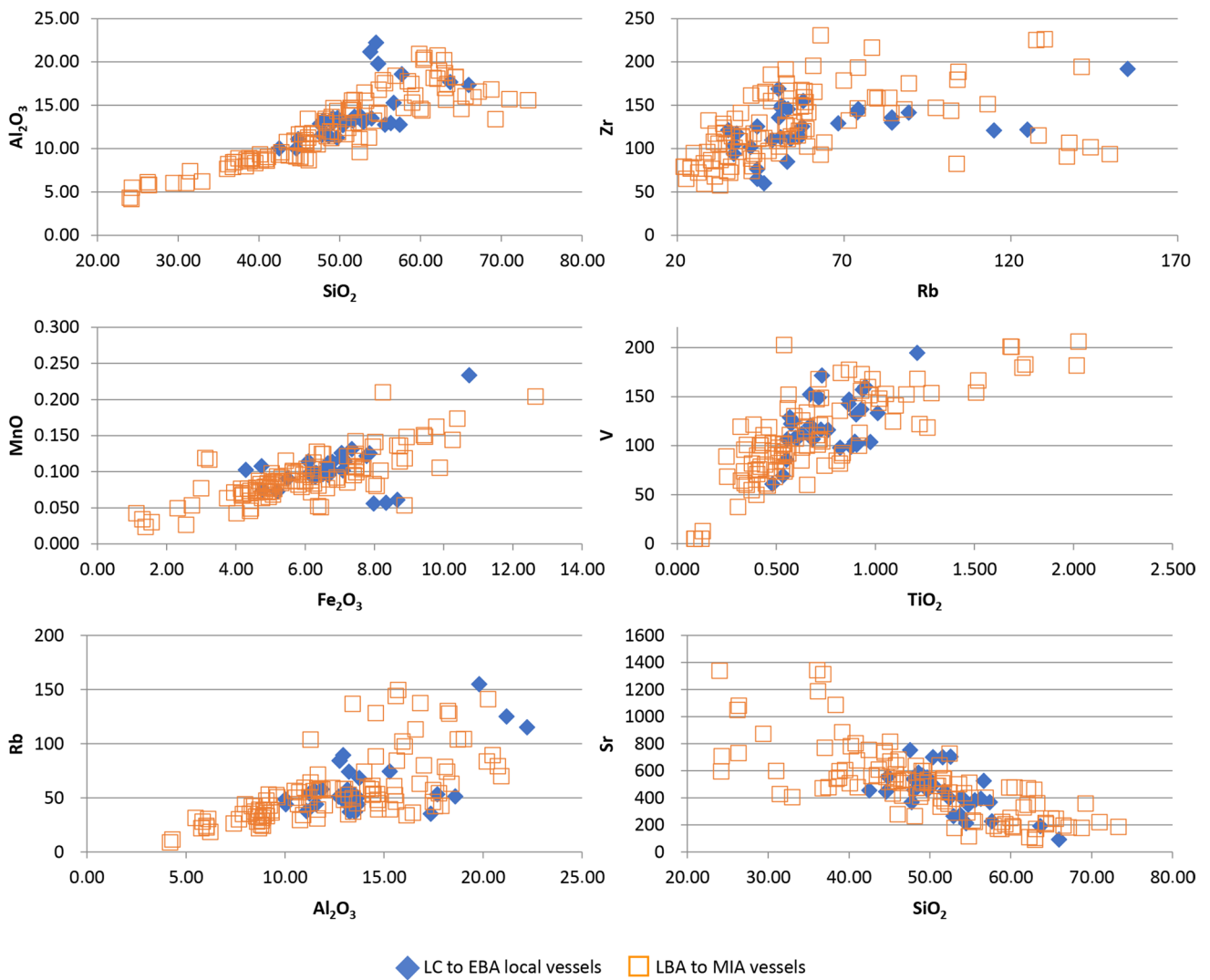
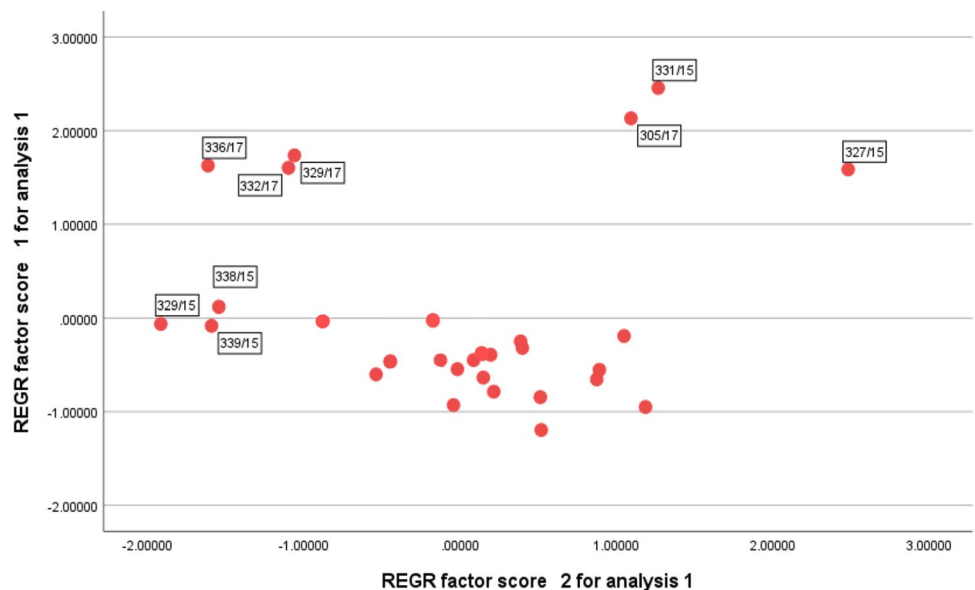


Fig. 12 Elemental binary plots showing the overlap between Late Bronze-Middle Iron Age sherds and the locally produced vessels of the previous phases

Fig. 13 Scatter plot of the principal component analysis relating factor 1 (47.2%: Al_2O_3 , -Ni, Fe_2O_3 , MgO, SiO_2 , -Sr, -Cr, TiO_2 , V) to factor 2 (19.4%: $-K_2O$, Ba, MnO, Rb)



durée. Coupled with preliminary observations on surface treatments and decorations, our data have also better clarified the impact of exogenous traditions on the local ones. In this perspective, future analyses will focus on exhaustively characterizing the materials, tools, and gestures involved in burnishing, slipping, and painting the surfaces of these same ceramic assemblages.

Acknowledgements The authors would like to express their gratitude to M. Frangipane (Rome) for her unwavering support and for granting permission to study the material from Arslantepe that is presented in this research. Additionally, the authors extend their appreciation to M. Sbrana (Servizi per la Geologia) for preparing the thin sections and to G. Schneider and M. Daskiewicz for conducting the XRFWDS analyses.

Author contribution Geological setting, materials and methods, thin-section petrography, discussion, XRFWDS geochemistry (Pamela Fragnoli); introduction, archeological and historical overview, pottery repertoire (Federico Manuelli); conclusions (Pamela Fragnoli, Federico Manuelli).

Funding Open access funding provided by Österreichische Akademie der Wissenschaften. The research project “Beyond the Crisis” (DFG Project #324049112) provided the necessary support for the completion of the current study. Excavations carried out at Arslantepe have been financially supported by Sapienza University of Rome and the Italian Ministry of Foreign Affairs. Research on the Iron Age levels has also benefited from a grant provided in 2016 by the National Geographic Society.

Data availability The images captured at Arslantepe are part of the archive of the Missione Archeologica Italiana in Anatolia Orientale (©MAIAO). The data and materials used during the study are available from the corresponding author upon reasonable requests.

Code availability Not applicable.

Declarations

Ethic approval The authors declare the integrity of the scientific record.

Consent to participate Both authors read, reviewed, edited, and approved the manuscript.

Consent for publication All authors agree with the submission to Archaeological and Anthropological Sciences.

Conflict of interest The authors declare no competing interests.

Open Access This article is licensed under a Creative Commons Attribution 4.0 International License, which permits use, sharing, adaptation, distribution and reproduction in any medium or format, as long as you give appropriate credit to the original author(s) and the source, provide a link to the Creative Commons licence, and indicate if changes were made. The images or other third party material in this article are included in the article's Creative Commons licence, unless indicated otherwise in a credit line to the material. If material is not included in the article's Creative Commons licence and your intended use is not permitted by statutory regulation or exceeds the permitted use, you will need to obtain permission directly from the copyright holder. To view a copy of this licence, visit <http://creativecommons.org/licenses/by/4.0/>.

References

- Alvaro C (2012) The topography and architecture at Arslantepe during the second and first millennia BC: reconsidering more than 100 years of research. In: Frangipane M (ed) Fifty years of excavations and researches at Arslantepe – Malatya (Turkey), Proceeding of the conference held at Rome, 5th-8th December 2011. Gangemi, Rome, pp 345–360
- Batmaz A (2020) A study of Urartian Red Glossy Pottery Production in Van, Turkey, using archaeological, ethnoarchaeological and experimental archaeological methods. *Ethnoarchaeology* 11(1):34–60. <https://doi.org/10.1080/19442890.2019.1573283>
- Baxter MJ (1994) Exploratory multivariate analysis in archaeology. Edinburgh University Press, Edinburgh
- Baxter MJ (1995) Standardization and transformation in principal component analysis, with applications to archaeometry. *Appl Stat* 44:513–527
- Baxter MJ (2003a) Statistics in Archaeology. Arnold, London
- Baxter MJ (2003b) Distance and transformation in the multivariate analysis of the archaeometric data. In: Martini M, Milazzo M, Placentini M (eds) Physics methods in archaeometry. Proceedings of the international school of physics “Enrico Fermi” (Villa Monastero, 17–27 June 2003), IOS Press, Amsterdam pp 17–37
- Ben-Shlomo D (2019) Cooking pot production in Judah during the Iron Age II. *Judea and Samaria Research Studies* 28(1):5–36. <https://doi.org/10.26351/JSRS/28-1/6>
- Blaylock S (2016) Tille höyük 3.2. The iron age: Pottery, objects and conclusions. The british institute of archaeology, London
- Bozkaya Ö, Yalçın H, Başibüyük Z, Özfırat O, Yılmaz H (2007) Origin and evolution of the southeast Anatolian metamorphic complex (Turkey). *Geol Carpath* 58(3):197–210
- D’Alfonso L, Basso E, Castellano L, Mantovan A, Vertuani P (2022) Regional exchange and exclusive elite rituals in Iron Age central Anatolia: dating, function and circulation of Alişar-IV ware. *Anatolian Studies* 72:37–77. <https://doi.org/10.1017/S0066154622000035>
- De Martino S (2012) Malatya and Işuwa in Hittite texts: new elements of discussion. In: Frangipane M (ed) Fifty years of excavations and researches at Arslantepe – Malatya (Turkey), Proceeding of the conference held at Rome, 5th-8th December 2011. Gangemi, Rome, pp 375–383
- Delaporte L (1940) Malatya: Fouilles de la mission archéologique française. Arslantepe, La Porte des Lions. De Boccard, Paris
- Fragnoli P (2018) Pottery production in pastoral communities: archaeometric analysis on the LC3-EBA1 Handmade Burnished Ware from Arslantepe (in the Anatolian Upper Euphrates). *J Archaeol Sci Rep* 18(4):318–332. <https://doi.org/10.1016/j.jasrep.2018.01.029>
- Fragnoli P, Frangipane M (2022) Centralisation and decentralisation processes and pottery production at Arslantepe (SE Anatolia) during the 4th and early 3rd millennium BCE. *World Archaeol* 53(5):834–861. <https://doi.org/10.1080/00438243.2021.2015623>
- Fragnoli P, Liberotti G (2019) Cross-craft strategies in raw material procurement: ceramics, mud bricks and other clay-based artefacts. In: Balossi Restelli F (ed) Arslantepe. Period VII. The development of a ceremonial/political centre in the first half of the fourth millennium BCE (Late chalcolithic 3-4), Arslantepe series II. Sapienza Università di Roma, Rome, pp 367–380
- Fragnoli P, Palmieri AM (2017) Petrographic and geochemical investigations on the pottery production from Arslantepe-Malatya (Eastern Anatolia) from the fourth to the second millennium BCE: Technological continuity, innovation and cultural change. *Archaeometry* 59(4):612–641. <https://doi.org/10.1111/arc.12266>

- Fragnoli P, Rodler AS (2022) Archaeometric and technological investigations of the Late Bronze Age painted pottery from Arslantepe (Malatya, eastern Turkey). In: Manuelli F, Mielke DP (eds) Late Bronze Age painted pottery traditions at the margins of the Hittite State. Proceedings of the Workshop Held at the 11th ICAANE (Munich, 4th of April 2019). Archaeopress, Oxford, pp 233–247
- Fragnoli P (2019a) (Re)defining ceramic wares and spheres of production in Arslantepe's period VII. The contribution of petrographic and geochemical analyses. In: Balossi Restelli F (ed) Arslantepe. Period VII. The development of a ceremonial/political centre in the first half of the fourth millennium BCE (Late Chalcolithic 3–4), Arslantepe Series II. Sapienza Università di Roma, Rome 357–367
- Fragnoli P (2019b) The introduction of the potter wheel in Arslantepe's period VII: Integrated observations on a micro-, meso- and macro-scale level. In: Balossi Restelli F (ed) Arslantepe. Period VII. The development of a ceremonial/political centre in the first half of the fourth millennium BCE (Late Chalcolithic 3–4), Arslantepe Series II. Sapienza Università di Roma, Rome, pp 345–357
- Frangipane M, Balossi Restelli F, Di Filippo F, Manuelli F, Mori L (2020) Arslantepe: new data on the formation of the Neo-Hittite Kingdom of Melid. *News from the Lands of the Hittites* 3–4:71–111
- Frangipane M, Palmieri A (1983) A protourban centre of the late uruk period. In: Frangipane M, Palmieri A (eds) Perspectives on protourbanization in Eastern Anatolia: Arslantepe (Malatya). An interim report on 1975–1983 campaigns. Gangemi, Rome, pp 287–454
- Frangipane M (2019) Arslantepe. The rise and development of a political centre: From temple to palace to a fortified citadel. In: Durak N, Frangipane M (eds) Arslantepe. Proceedings of the I. International archaeology symposium. İnönü Üniversitesi Matbaası, Malatya, pp 71–104
- Freestone IC, Meeks ND, Middleton AP (1985) Retention of phosphate in buried ceramics: an electron microbeam approach. *Archaeometry* 27:161–177
- Gilboa A (2015) Iron age I-II cypriot imports and local imitations. In: Aviram J, Ben-Tor A, Stern E, Yannai E (eds) The ancient pottery of Israel and its neighbors. From the iron age through the hellenistic period Vol. 2. Israel exploration society, Jerusalem pp 483–508
- Glascok MD (1992) Characterization of archaeological ceramics at MURR by neutron activation analysis and multivariate statistics. In: Neff H (ed) Chemical characterization of ceramic pastes in archaeology. Prehistory Press, Madison, pp 11–26
- Hawkins JD (2000) Corpus of hieroglyphic luwian inscriptions: Vol. 1. Inscriptions of the iron age. De Gruyter, Berlin
- Kibaroglu M, Kozal E, Klügel A, Hartmann G, Monien P (2019) New evidence on the provenience of Red Lustrous Wheel-made Ware (RLW): petrographic, element and Sr-Nd isotope analysis. *Journal of Archaeological Science: Report* 24:412–433. <https://doi.org/10.1016/j.jasrep.2019.02.004>
- Liverani M (2010) Il salone a pilastri della melid neo-hittita. *Scienze dell'Antichità* 15:649–775
- Liverani M (2012) Arslantepe in the Neo-Hittite Period. In: Frangipane M (ed) Fifty years of excavations and researches at Arslantepe – Malatya (Turkey), Proceedings of the conference held at Rome, 5th–8th December 2011. Gangemi, Rome pp 331–344
- Manuelli F (2018) Drifting southward? Tracing aspects of cultural continuity and change in the late 2nd millennium BC Syro-Anatolian region. *Studia Eblaitica* 4:139–186
- Manuelli F (2020) The regeneration of the Late Bronze Age traditions and the formation of the Kingdom of Malizi. In: Sonne A (ed) Formation, organization and development of the Iron Age societies. Österreichischen Akademie der Wissenschaften, Vienna, pp 109–129
- Manuelli F, Mori L (2016) The King at the Gate Monumental fortifications and the rise of local elites at Arslantepe at the end of the 2nd millennium BCE. *Origini* 39(1):209–241
- Manuelli F, Vignola C, Marzaioli F, Passariello I, Terrasi F (2021) The beginning of the Iron Age at Arslantepe: a 14C perspective. *Radiocarbon* 63(3):885–903. <https://doi.org/10.1017/RDC.2021.19>
- Manuelli F (2013) Arslantepe IX. Late bronze age. Hittite influence and local traditions in an eastern anatolian community, Arslantepe series IX. Sapienza university of Rome, Rome
- Manuelli F (2022) Just a matter of style? Late bronze age painted pottery traditions in the Upper Euphrates region: Origins and significance. In: Manuelli F, Mielke DP (eds) Late bronze age painted pottery traditions at the margins of the hittite state. Proceedings of the workshop held at the 11th ICAANE (Munich, 4th of April 2019). Archaeopress, Oxford pp 204–232
- Mielke DP (2007) Red lustrous wheelmade ware from hittite contexts. In: Hein I (ed) The lustrous wares of the late bronze age cyprus and the eastern mediterranean. Paper of a conference held at the Austrian academy of sciences, Vienna, 5th–6th November 2004. Österreichischen Akademie der Wissenschaften, Vienna pp 155–168
- Mielke DP, Kibaroglu M, Behrendt S, Viehhaus T (2021) Archäometrische charakterisierung einer neu entdeckten keramikgattung aus der spätbronzezeit anatoliens. *Metalla Sonderheft* 11:52–54
- Mineral Research and Exploration (MTA) (2002) 1/500.000 scale geological maps of Turkey, General Directorate of Mineral Research and Exploration (MTA), Ankara, Turkey
- Ökse AT (1988) Mitteleisenzeitliche Keramik Zentral-Ostanatoliens mit dem Schwerpunkt Karakaya-Staudammgebiet am Euphrat. PeWe Verlag, Berlin
- Önal A (2008) Mineral chemistry crystallization condition and magma mixing-mingling at Orduzu Volcano (Malatya), Eastern Anatolia, Turkey. *Geol J* 43:5–116. <https://doi.org/10.1002/gj.1105>
- Önal A, Boztuğ D, Arslan M, Spell LT, Kürüm S (2008) Petrology and ⁴⁰Ar/³⁹Ar age of the bimodal Orduzu volcanic (Malatya) from the western end of the eastern Anatolian Neogene volcanism, Turkey, Turkish. *Journal of Earth Sciences* 17:85–109
- Osborne JF (2021) The Syro-Anatolian City-States. Oxford University Press, Oxford, An Iron Age culture
- Palmieri A (1973) Scavi nell'area sud-occidentale di Arslantepe. Ritrovamento di una struttura templare dell'Antica Età del Bronzo. *Origini* 7:55–228
- Palmieri A (1978a) Scavi ad arslantepe (Malatya). *Quaderni de "La Ricerca Scientifica"* 100:311–373
- Palmieri AM (1978b) Studio sedimentologico dell'area nord-occidentale di Arslantepe. *Quaderni de "La Ricerca Scientifica"* 100:353–364
- Parlak O, Karaoğlan F, Rızaoğlu T, Nurlu N, Bağcı U, Höck V, Öztü A, Önal F, Kürü S, Topak Y (2012) Petrology of the İspendere (Malatya) ophiolite from the Southeast Anatolia: implications for the Late Mesozoic evolution of the southern Neotethyan Ocean. Geological Society, Special Publications Published Online. <https://doi.org/10.1144/SP372.11>
- Pecorella PE (1975) Malatya – III. Rapporto preliminare delle campagne 1963–1968. Il livello eteo imperiale e quelli neoetei. Centro per le antichità e la storia dell'arte del Vicino Oriente, Rome
- Rice PM (1987) Pottery analysis: a sourcebook. The University of Chicago Press, Chicago
- Robertson AHF, Ustaömer T, Parlak O, Ünlügenç UC, Taslı K, İnan N (2006) The Berit transect of the Tauride Thrust Belt, S. Turkey: Late Cretaceous–Early Cenozoic accretionary/collisional processes related to closure of the Southern Neotethys. *J Asian Earth Sci* 27:108–145. <https://doi.org/10.1016/j.jseaes.2005.02.004>
- Sarıfakıoğlu E, Dilek Y, Sevin M (2014) Jurassic–Paleogene intraoceanic magmatic evolution of the Ankara Mélange, north-central

- Anatolia, Turkey. *Solid Earth* 5:77–108. <https://doi.org/10.5194/se-5-77-2014>
- Şaşmaz A, Turkyılmaz B, Öztürk N, Yavuz F, Kumral M (2014) Geology and geochemistry of middle Eocene Maden Complex ferromanganese deposits from the Elaziğ-Malatya region, Eastern Turkey. *Ore Geol Rev* 56:352–372. <https://doi.org/10.1016/j.oregeorev.2013.06.012>
- Schwedt A, Mommsen H, Zacharias N (2004) Post-depositional elemental alterations in pottery activation analysis of surface samples. *Archaeometry* 46(1):85–101. <https://doi.org/10.1111/j.1475-4754.2004.00145.x>
- Soldi S (2013) Red slip ware from the acropolis of tell afis: The evidence of area G. In: Mazzoni S, Soldi S (eds) *Syrian archaeology in perspective. Celebrating 20 years of excavations at Tell Afis*. Edizioni ETS, Pisa, pp 199–222
- Vignola C, Marzaioli F, Balossi Restelli F, Di Nocera GM, Frangipane M, Masi A, Passariello I, Sadori L, Terrasi F (2019) Changes in the Near Eastern Chronology between the 5th and the 3rd Millennium BC: new AMS 14C dates from Arslantepe (Turkey). *Nucl Instrum Methods Phys Res, Sect B* 456:276–282. <https://doi.org/10.1016/j.nimb.2019.01.033>
- Yazgan E, Mason R (1988) Orbicular gabbro near Baskil, Southeastern Turkey. *Mineral Mag* 52:161–173
- Yiğitbaş E, Yılmaz Y (1996) New evidence and solution to the Maden Complex controversy of the southeast Anatolian orogenic belt (Turkey). *Geol Rundsch* 85:250–263

Publisher's note Springer Nature remains neutral with regard to jurisdictional claims in published maps and institutional affiliations.